SPECIAL PUBLICATIONS OF THE INTERNATIONAL UNION OF GEODESY AND GEOPHYSICS

IUGG
UGGI

Dynamics and Predictability of Large-Scale, High-Impact Weather and Climate Events

Edited by **Jianping Li, Richard Swinbank, Richard Grotjahn, and Hans Volkert**

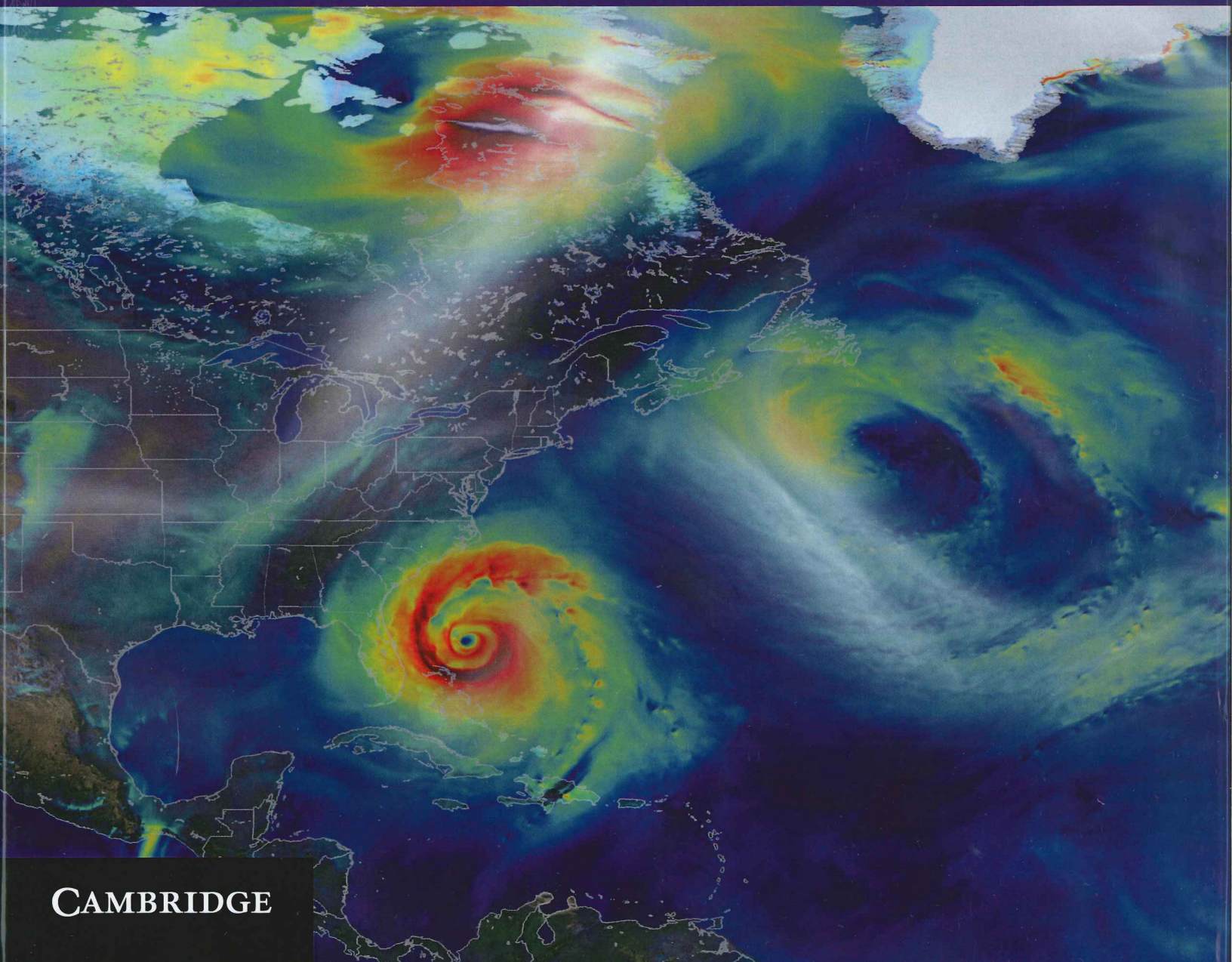

CAMBRIDGE

21

Key role of the Atlantic Multidecadal Oscillation in twentieth century drought and wet periods over the US Great Plains and the Sahel

Sumant Nigam and Alfredo Ruiz-Barradas

21.1 Introduction

Sea surface temperatures (SST) exert a significant, and often predictable, influence on the climate of near and far away regions. Interannual SST variations related to El Niño Southern Oscillation (ENSO), for instance, impact the Indian summer monsoon to the west (Rasmusson and Carpenter, 1983) and the North American hydroclimate to the east (e.g. Ropelewski and Halpert, 1987, Joseph and Nigam, 2006). The link between SST and hydroclimate is also manifest on decadal time scales, as in the case of droughts over North America (Namias, 1966, Ting and Wang, 1997, Nigam *et al.*, 1999) and Africa (Hulme, 1992). Multi-year droughts such as the 1930s 'Dust Bowl'[2] over the Great Plains, and the multi-decade 'drying' of Sahel (Folland *et al.*, 1986) mark notable excursions of regional hydroclimate, with devastating socioeconomic impacts. Such decadal-scale excursions, rooted in ocean–atmosphere–land interaction, are attractive targets for climate simulation and prediction for societal and scientific reasons.[3]

Multi-year, summertime droughts over North America have been observationally linked to decadal SST variability in the Pacific (Ting and Wang, 1997, Nigam *et al.*, 1999, Barlow *et al.*, 2001, McCabe *et al.*, 2004, White *et al.*, 2008, Nigam *et al.*, 2011) and the Atlantic (Namias, 1966, McCabe *et al.*, 2004, Ruiz-Barradas and Nigam, 2005, Wang *et al.*, 2006, Guan, 2008, McCabe *et al.*, 2008, Mo *et al.*, 2009, Nigam *et al.*, 2011) but the extent of the SST influence in major twentieth century droughts (including basin contributions) remained unevaluated, observationally, until the attribution analysis of Nigam et al. (2011).

The drying of the Sahel has been attributed to local land-surface–atmosphere interaction – the overgrazing hypothesis (Charney, 1976, Charney and Stone, 1976) – and to tropical Atlantic and global SSTs (Folland *et al.*, 1986, Giannini *et al.*, 2003, Zhang and Delworth, 2006), global warming (Held *et al.* 2005) and recently to anthropogenic aerosols (Biasutti and Giannini, 2008).

Droughts are typically simulated using dynamical models of the atmosphere. The models are forced by observed SST which provides the temporal context, including drought links. The SST influence can be dynamically evaluated from a sufficiently large ensemble of drought simulations provided the atmospheric–land-surface model is realistic, at least, from the perspective of the hydroclimate variability structure (and mechanisms) of the target region. The currently deployed atmospheric models (Schubert *et al.*, 2004, Seager *et al.*, 2005, Sutton and Hodson, 2005, Cook *et al.*, 2009, Schubert *et al.*, 2009) simulate many aspects of the atmospheric general circulation, but the simulation of regional hydroclimate (precipitation, evaporation/evapotranspiration, soil moisture, surface air temperature, etc.) remains challenging. The problematic portrayal includes a distorted representation of the atmospheric and terrestrial water-cycles over the Great Plains (Ruiz-Barradas and Nigam, 2005, Nigam and Ruiz-Barradas, 2006, Ruiz-Barradas and Nigam, 2013), i.e. of regional processes relevant to droughts (Ruiz-Barradas and Nigam, 2010a,b).

In spite of such shortcomings, aspects of the notable Great Plains droughts have been simulated by SST-forced dynamical models. But the modeled drought core is often misplaced, e.g. to the southwest in the case of the Dust Bowl drought (Seager *et al.*, 2005, Cook *et al.*, 2009). The modeled drought is moreover characterized using *annual-mean* precipitation deficits in these studies, which downplays the hydroclimate simulation deficiencies of the warm season (late spring to fall) – the season of drought

[2] The intense decade-long (1931–39) drought got its name on 15 April 1935, the day after Black Sunday. Robert Geiger, a reporter for the Associated Press, travelled through the region and wrote the following: "Three little words achingly familiar on a Western farmer's tongue, rule life in the *dust bowl* of the continent-if it rains."

[3] Decadal prediction of regional hydroclimate, especially in the hind cast mode, provides unique opportunities for vetting climate system models used in projection of centennial-scale climate change.

occurrence over the Great Plains.[4] The modeled drought signal, as such, reflects more the La Niña footprint on winter–spring precipitation (Seager *et al.*, 2005) than the larger precipitation deficits observed in the warm season. Some notable North American droughts are, moreover, conspicuously absent while others fictitiously present in some of the simulations (Schubert *et al.*, 2004). Do the drought simulation discrepancies reflect the limited influence of SSTs in models or nature?

North American droughts are more strongly linked with the Pacific than Atlantic SST anomalies in dynamical model simulations (e.g. Figure 3 in Schubert *et al.*, 2004); the Pacific influence resulting, largely, from tropical SST anomalies (Schubert *et al.*, 2004, Seager *et al.*, 2005). The coordinated modeling experiments of the US CLIVAR Drought Working Group (Schubert *et al.*, 2009) reiterate the primacy of Pacific SSTs in generating North American droughts. The La Niña – US Drought paradigm – operative on interannual time scales in nature – was found most relevant in the context of decadal droughts by these modeling studies.

How does one define the simulation targets for the SST-based dynamical modeling of droughts? Clearly, the targets are not the full observed drought signal in view of the land-surface contribution: Are the models being judged too harshly above? Or are the present-day models not quite ready for scoping out the influence of Pacific and Atlantic SSTs on Great Plains and Sahel's precipitation?

The goal of this observationally rooted analysis is to quantitatively characterize the full SST contribution in drought generation over North America and Africa, including the relative role of the Pacific and Atlantic basins. The characterization closely follows Nigam *et al.* (2011), where an evolution-centric spatiotemporal analysis of twentieth century SST variations (Guan and Nigam, 2008, 2009) and related hydroclimate links, and subsequent reconstruction of North American droughts yield the impact of Pacific and Atlantic SST variations on continental hydroclimate. The observationally based impacts immediately provide the sought after quantitative targets for the SST-forced dynamical modeling of droughts.

The observationally rooted statistical reconstruction of major hydroclimate episodes in Nigam *et al.* (2011) indicates a dominant role of Atlantic SSTs in the generation of multi-year droughts and wet episodes over North America – in contrast with the secondary role of this basin in model-based assessments. The Atlantic Multidecadal Oscillation (AMO), in particular, had a singular influence on the twentieth century North American hydroclimate, especially during spring and fall, as discussed in subsequent sections. The AMO is a dominant contributor in the drying of the Sahel from the 1950s to the 1980s as well, and in the recovery of rainfall since.

Data sets are described in Section 21.2, and the notable hydroclimate episodes of the twentieth century in Section 21.3. The enabling SST analysis is briefly discussed in Section 21.4. The drought-period SST and precipitation signals are reconstructed from contemporaneous analysis in Section 21.5, while the Great Plains drought origin and predictability are investigated in Section 21.6. The drying of the Sahel is reconstructed in Section 21.7 to assess the influence of regional and remote SSTs. Discussions and conclusions follow in Section 21.8.

21.2 Data sets

The sea surface temperature data comes from the UK Met Office's Hadley Centre Sea Ice and Sea Surface Temperature data set (HadISST 1.1, Rayner *et al.*, 2003), which is globally available on a 1° grid for the 1870-onward period. The long-term mean of each calendar month is first removed from the monthly data, yielding monthly anomalies. Seasonal anomalies are then constructed by averaging monthly anomalies over standard three-month periods (e.g., DJF, JJA). Seasonal anomalies are interpolated on to a 5° × 2.5° longitude–latitude grid for computational efficiency in extended-EOF analysis.

Precipitation data is from the University of East Anglia's Climate Research Unit (CRU); the high resolution TS 3.0 analysis of station data (Mitchell and Jones, 2005). Monthly precipitation is available over land on a 0.5° grid for the 1901 onward period.

The Palmer Drought Severity Index, a nondimensional number that measures the severity of meteorological drought, is obtained from Dai *et al.*'s (2004) analysis. Monthly PDSI is available over land regions on a 2.5° grid for the 1870 onward period.

Evapotranspiration estimates are obtained from NOAA's Climate Prediction Center, where they are generated using a one-layer hydrological model (Huang *et al.*, 1996, van den Dool *et al.*, 2003) that is driven by observed precipitation (and surface air temperature). Monthly evaporation is available on a 2.5° grid for the 1931 onward period.

Upper-air meteorological analysis for the full century was obtained from NOAA's Twentieth Century Reanalysis (20CR; Compo *et al.*, 2011), which was developed from short-term forecasts generated from assimilation of synoptic surface/sea-level pressure and monthly SST and

[4] The downplay results from the comparatively superior simulation of winter hydroclimate variability which is dynamically controlled (through stormtrack modulation). Warm-season hydroclimate variability, in contrast, is more influenced by land-surface–atmosphere interactions which are robust (dormant) in summer (winter) but which remain poorly rendered in atmospheric and climate models.

sea-ice boundary conditions. The modern period upper-air data comes from NOAA's NCEP Reanalysis (Kalnay *et al.*, 1996).

21.3 Notable hydroclimate episodes of the twentieth century

The hydroclimate of the US Great Plains is marked by two notable dry periods in the twentieth century (Fig. 21.1a): one in the 1930s and the other in the 1950s. The 1930s drought was intense and prolonged (decade-long), and turned much of the Great Plains, the US breadbasket, into a 'Dust Bowl'. The 1950s drought, while relatively short (4–5 years), was no less intense; its fall precipitation deficit was, in fact, larger than the peak seasonal deficit during the Dust Bowl drought (Fig. 21.1b–c). The1950s drought was unrelenting as well, as is evident from the complete absence of positive precipitation anomalies (in any season) during the episode (Fig. 21.1a), in contrast with the distribution in Dust Bowl years. The 'Dust Bowl' winters, interestingly, had near-normal precipitation, on average; a feature, not evident in descriptions based on the Palmer Drought Severity Index (PDSI; Palmer, 1966). Droughts are commonly marked using the PDSI but this index is, seasonally, less discriminating than a precipitation based one (Fig. 21.1b–d), and thus not as insightful on drought mechanisms which are keyed to seasonal process.[5]

The Dust Bowl was largely a spring–summer drought while the 1950s one a summer–fall drought (Fig. 21.1b–c). The Great Plains precipitation record also includes wet periods, with a notable one in the mid 1980s that is focused on fall (Fig. 21.1d). Regional evapotranspiration anomalies (Fig. 21.1b–d) are largest in summer following the climatological rhythm, but never sufficient to account for even half the concurrent precipitation deficits, especially in the peak phase of the episodes – indicating, indirectly, a significant role for larger-scale circulation variations and attendant moisture transports in modulating the water cycle over the Great Plains (Ruiz-Barradas and Nigam, 2005).

Geographically, the Dust Bowl precipitation deficit is focused in the southern Plains and along the Gulf Coast in spring and in the central-northern Plains in summer (Fig. 21.1e–f). Drought severity can be assessed by comparing the precipitation deficit in the box outlined in Fig. 21.1f (~0.6 mm/day) with the regional summer climatology (~3.0 mm/day) (e.g. Nigam and Ruiz-Barradas, 2006) and standard deviation (~0.9 mm/day) (e.g. Ruiz-Barradas and Nigam, 2005). The 1950s fall drought was more intense (~1.0 mm/day deficit against a fall climatology of ~2.7 mm/day and standard deviation of ~1.0 mm/day) and widespread, with the entire USA impacted (Fig. 21.1g). The drought core is located southward, extending into the southern Plains and the Gulf Coast states. The 1980s wet episode is essentially a mirror image of the 1950 drought, in both structure and amplitude; not surprising, given that both attain their peak-phase in the fall.

The Pacific SSTs during the Dust Bowl spring and summer were, on average, colder, especially in the extra-tropics, although not by much (~0.3 K) (Fig. 21.2a–b); the tropics, interestingly, were near normal. In contrast, robustly warm SSTs are found in the Atlantic, especially in summer when most of the mid-latitude basin has large SST anomalies (0.5–0.8 K); the tropical Atlantic is mildly warmer as well. The cold SST anomalies in the central-eastern equatorial Pacific during the 1950s fall drought (Fig. 21.2c) clearly resemble the La Niña signal [e.g. Fig. 3 (right panels) in Guan and Nigam (2008), in the opposite phase. The Atlantic anomalies in the 1980s wet period (Fig. 21.2d) are broadly a mirror image of the drought ones, while the Pacific ones are more fragmented at this time.

21.4 The enabling SST analysis

The drought reconstruction reported here is rooted in the innovative analysis of natural variability and secular trend in the Pacific and Atlantic SSTs in the twentieth century (Guan and Nigam 2008, 2009; hereafter GN2008 and GN2009). By focusing on spatial *and* temporal recurrence but without imposition of any periodicity constraints, the extended empirical orthogonal function analysis (EEOF; Weare and Nasstrom, 1982) discriminates between biennial, interannual, and decadal variabilities, leading to refined evolutionary descriptions and, equally importantly, separation of natural variability and the secular trend – all without any advance filtering (and potential aliasing) of the SST record. The implicit accommodation of natural variability, in particular, leads to a nonstationary SST secular trend, one that includes mid-century cooling.

21.4.1 Pacific analysis

Seasonal SST anomalies between 1900 and 2007 were analyzed in the Pan-Pacific domain (20°S–60°N, 120°E–60°W) using the EEOF technique; five-season-long anomaly sequences were targeted in the primary analysis. The technique is equivalent to multichannel singular spectrum analysis (e.g. von Storch and Zwiers, 1999). The seven

[5] Smoothed versions of PDSI can moreover be synthesized from precipitation, indicating the latter's adequacy in multi-year drought analysis; smoothed precipitation and PDSI indices are correlated at 0.91 in Fig. 21.1a.

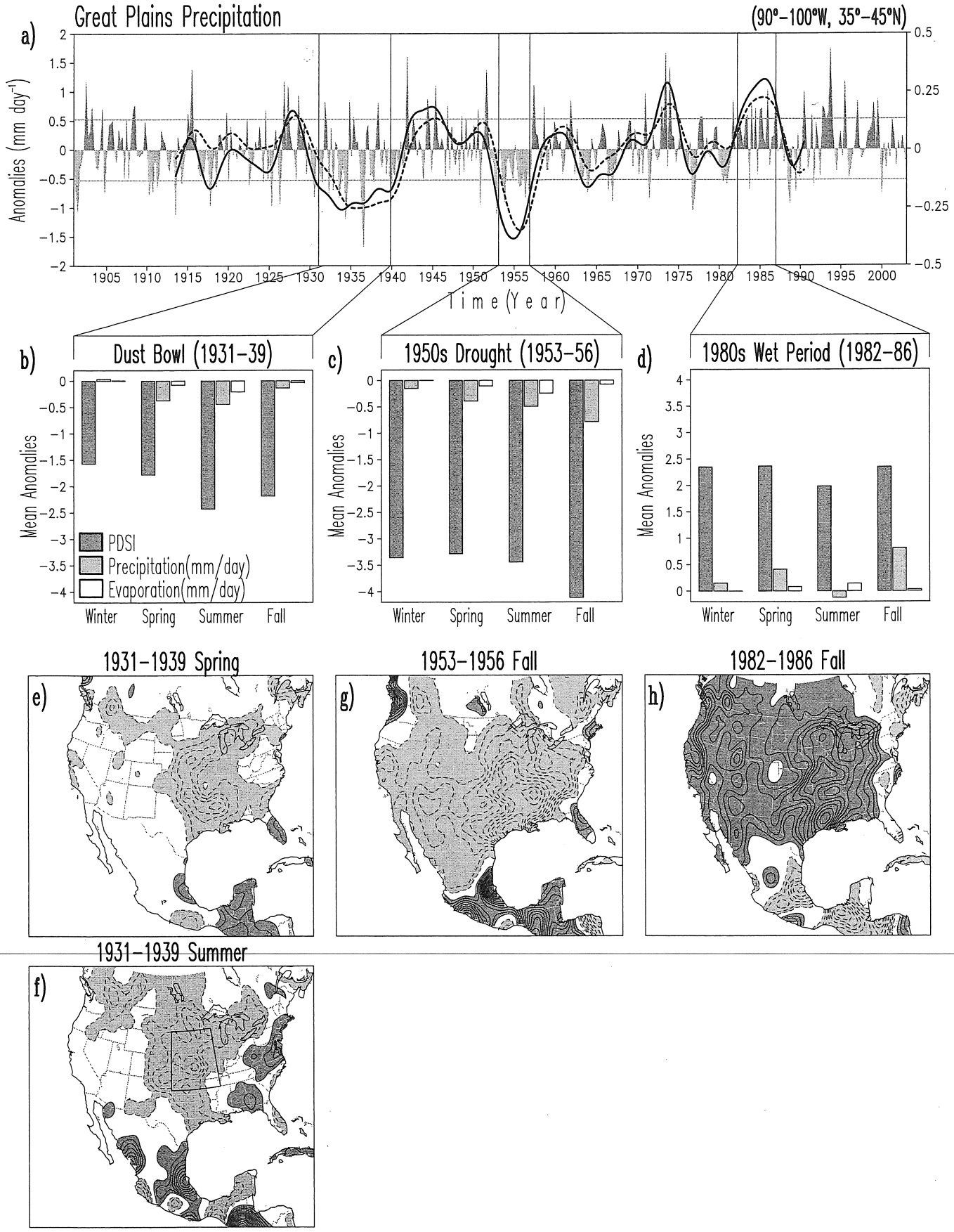

Fig. 21.1. North American drought and wet episodes: (A) Great Plains precipitation in the twentieth century, from Climate Research Unit's TS 3.01 data (University of East Anglia); averaging region (90°W–100°W, 35°N–45°N) outlined in (F). Seasonal anomalies (mm/day, left scale) are in green/brown shades; solid black line shows a smooth version (from 50 applications of 1-2-1 averaging)

leading principal components (PCs) were rotated using the VARIMAX method. Canonical ENSO variability is captured as two modes: growth ($ENSO^{-}$) and decay ($ENSO^{+}$); departures from it are identified as the non-canonical mode ($ENSO^{NC}$); see Figures 3–9 and related discussion in GN2008. Pacific decadal variability is resolved into two modes, Pan Pacific (PDV-PP) and North Pacific (PDV-NP): The first, with a horseshoe structure in the Pacific, exhibits connections to the tropical–subtropical Atlantic resembling the AMO footprint in this region (Figure 11 in GN2008). The second, capturing the 1976/77 climate shift, is closer to Pacific Decadal Oscillation in structure, but with interesting links to other basins (Figure 12 in GN2008). The nonstationary secular trend (SST-Trend) consists of widespread but nonuniform warming of all basins along with a sliver of cooling in the central equatorial Pacific (Figure 13 in GN2008). The physicality of decadal modes – of key interest given their multi-year drought links – was assessed via correlations with the fish recruitment records, following Hare and Mantua (2000); the correlations were found to be comparable, if not larger, than those obtained by these authors. Analog counts were also used in assessing the physicality of the modes (see Section 5 in GN2008).

21.4.2 Atlantic analysis

The Atlantic SSTs were subject to similar spatiotemporal analysis, but after removal of the Pacific influence. The leading mode of Atlantic SST variability is a multidecadal oscillation focused in the extratropical basin (AMO-*Atl*; GN2009). It differs from its conventional description (Enfield *et al.*, 2001, Enfield and Cid-Serrano, 2010) in the western tropical basin where the amplitude is weaker due to the absence of the Pacific's influence (see Figure 5b in GN2009). The seasonally resolved AMO-*Atl* PC is shown in Fig. 21.3a (thin red) along with other markers of this variability, including a recent one from Ting *et al.* (2009) based on observations and climate model simulations; note Fig. 21.3 is identical to Figure 1 in Nigam *et al.* (2011), and reproduced with permission. Negative decadal pulses reflecting massive discharge of sub-Arctic water into the North Atlantic, as during the Great Salinity Anomaly of 1968–82 (e.g. Slonosky *et al.*, 1997), are evident in the AMO-*Atl* PC (and to an extent in the Ting index) but not in other AMO markers; AMO-*Atl* differs from others in the1940s and 1950s too.

The AMO-*Atl*'s SST footprint (Fig. 21.3b) is focused in the northern basin, in the subpolar gyre. The same-sign extension into the Tropics develops a little after the northern lobe attains significant amplitude; AMO-*Atl* evolution is shown in GN2009. The fall-season regressions on land precipitation (Fig. 21.3b) show a general drying over the Americas (except southern Mexico and Central America), but wetter conditions to the east, notably, over Sahel. Given AMO-*Atl*'s decadal time scales, its warm phase can lead to multi-year droughts over central-eastern United States.

21.4.3 AMO-Atl's seasonal precipitation footprints

AMO-*Atl*'s impact on North American seasonal precipitation (Fig. 21.3c) is significant in the transitional and warm seasons, with the fall impact being largest (0.4–0.5 mm/day per unit PC amplitude). The AMO-*Atl*'s warm phase is associated with precipitation deficits in all three seasons; the absence of offsetting surpluses (or seasonal compensation) makes AMO-*Atl* even more relevant for North American droughts. The overlaid regressions of the 700 hPa geopotential and column stationary moisture flux (from a data set completely independent of CRU precipitation) indicate a strikingly consistent circulation context for the precipitation signal: low-level northerly flow across the central continent and related southward moisture transport. The flow opposes the seasonal southerly flow (including the Great Plains low-level jet in spring) which brings moisture from the Gulf of Mexico into the continental interior (e.g. Nigam and Ruiz-Barradas, 2006, Weaver and Nigam, 2008). The AMO-*Atl* circulation leads to a precipitation deficit both from reduced moisture transport and the low-level subsidence generated by northerly anomalies [assuming a Sverdrup vorticity balance, namely, $\beta.v \approx f\,(\partial w/\partial z)$].

Caption for Fig. 21.1 (*cont.*) using the right scale. Dashed line shows the Palmer Drought Severity Index anomalies (similarly smoothed but scaled by 0.1) using the same right scale. Horizontal lines mark the ±1.0 SD of the smoothed precipitation index. Vertical lines identify periods when this index exceeds ±1.0 SD. (B) Seasonal Palmer Drought Severity Index, precipitation, and evapotranspiration (from NOAA Climate Prediction Center, in mm/day) anomalies over the Great Plains in the Dust Bowl years (1931–39). (C) As in B except for the 1950s drought (1953–56). (D) As in B except for the 1980s wet period (1982–86). All anomalies in (B)–(D) are relative to the 1931–2002 seasonal climatology. Dust Bowl precipitation anomalies in Spring (E) and Summer (F). Fall precipitation anomalies in the 1950s drought (G) and 1980s wet period (H). Precipitation is smoothed by five applications of *'smth9'* in the GrADS plotting software, and displayed using a 0.15 mm/day interval; zero-contour is suppressed. Green (brown) shades denote positive (negative) values.

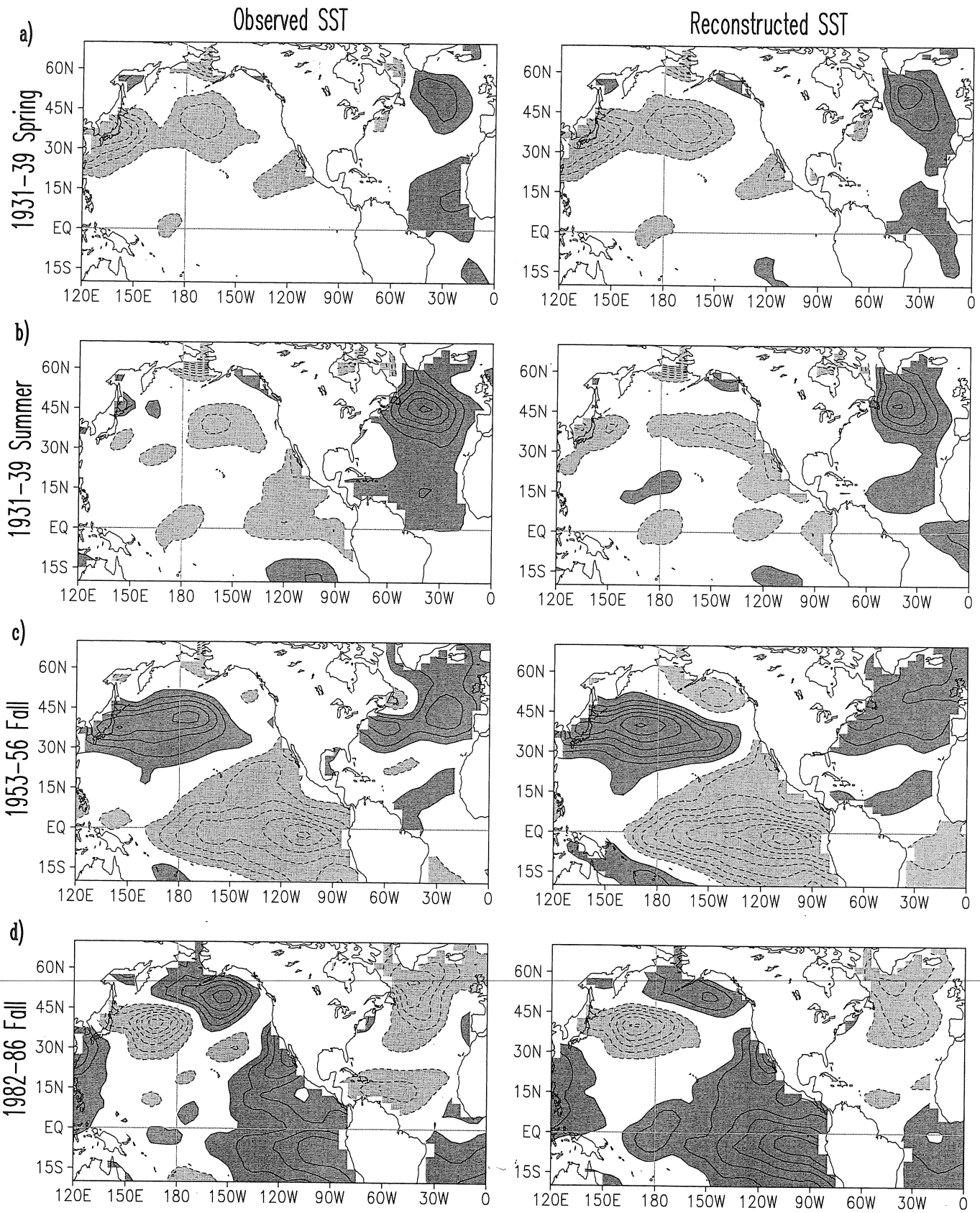

Fig. 21.2. Observed sea surface temperature anomalies during notable North American drought and wet episodes, from the Hadley Centre's HadISST 1.1 analysis (UK Meteorological Office); relative to the 1900–2002 period's seasonal climatology, and plotted on a 5° longitude by 2.5° latitude grid: (A) Dust Bowl (1931–39) spring, (B) Dust Bowl summer, (C) 1953–56 fall drought, and (D) the 1982–86 wet episode (fall). The SST anomalies reconstructed from seasonal regressions of the *seven* Pacific and *four* Atlantic SST principal components are shown in the right panels. Solid (dashed) contours denote positive (negative) values and the zero-contour is suppressed; contour interval is 0.15 K. Sea surface temperature is spatially smoothed by one application of *'smth9'* in the GrADS plotting software. Red (blue) shades denote positive (negative) values.

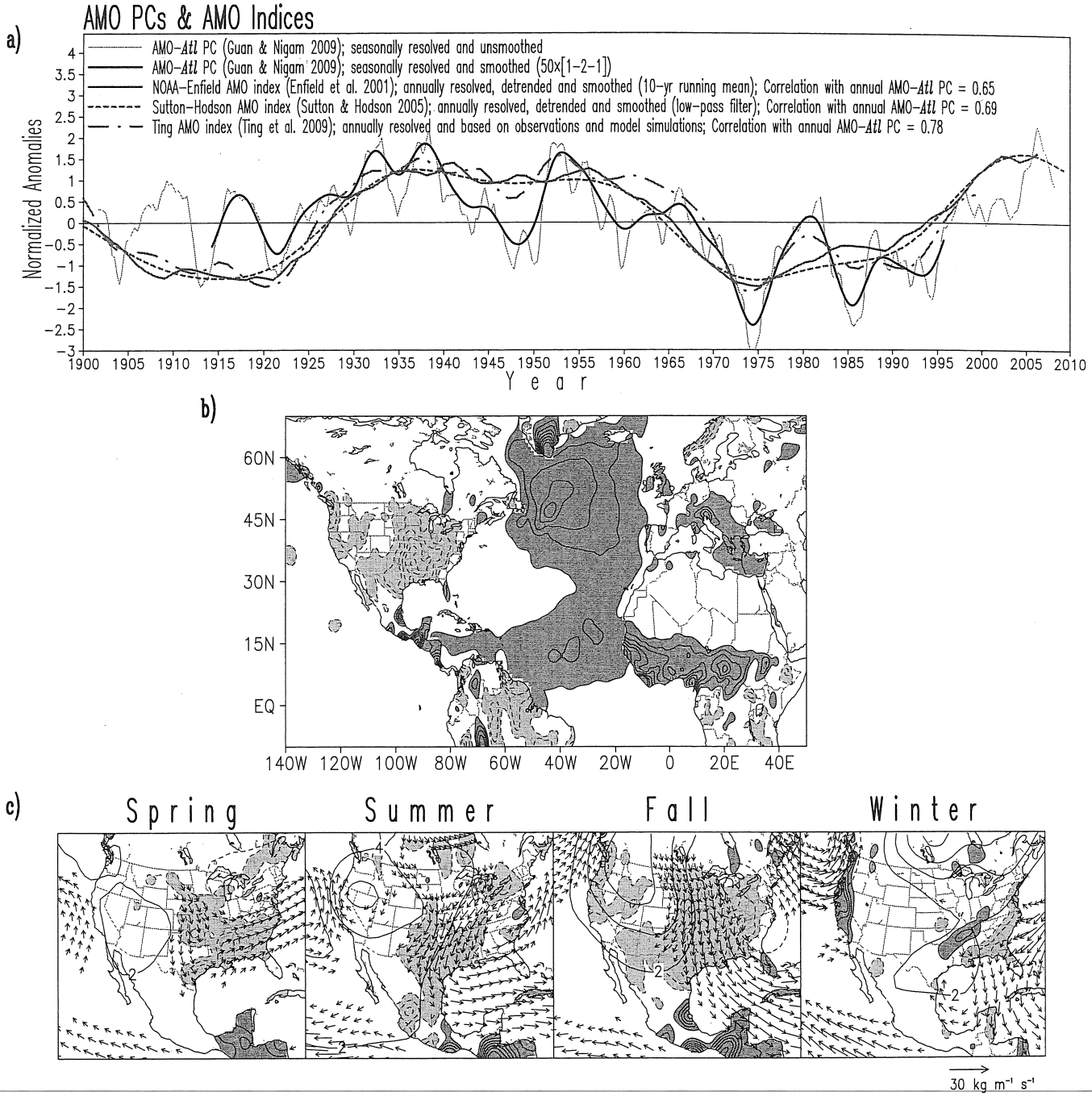

Fig. 21.3. (A) Atlantic Multidecadal Oscillation SST principal component (AMO-*Atl* PC, red) is compared with other AMO indices: NOAA-Enfield (black); Sutton-Hodson (green); and the Ting *et al.* index (purple-x). The notable 1970s decadal pulse in the AMO-*Atl* PC is coincident with the Great Salinity Anomaly (see text). The smoothed PC (thick red) is obtained from 50 applications of the 1-2-1 smoother on seasonally resolved values (thin red); all indices are normalized over the January 1900–April 2009 period. Smoothed index correlations: (Red, Black)=0.65; (Red, Green)=0.69; (Red, Purple)=0.78. (B) All-season regressions of the smoothed AMO-*Atl* PC on *residual* Atlantic SSTs (see text for definition) are shaded blue-to-red while its *fall*-season regressions on precipitation are shown in brown-to-green colors. SST is contoured at 0.1 C intervals and precipitation is shaded/contoured at 0.075 mm/day. (C) AMO's impact on North American *seasonal* hydroclimate: Regressions of smoothed AMO-*Atl* PC on precipitation, and NOAA-20CR's 700 hPa geopotential and surface-300 hPa column stationary moisture flux. Precipitation is plotted as above, height is contoured at 2 m, and the column moisture flux is in blue vectors with the indicated scale (in kg $m^{-1}s^{-1}$), and with values less than 15% of the scale not plotted; zero contours are omitted in all panels. All regressions are for the April 1914–July 1995 period, the interval over which the thick red curve (panel a) is defined. To preclude aliasing of the nonstationary SST Secular Trend PC in the regressions, its signal in seasonal data was removed prior to regression analysis; smoothing of the AMO-*Atl* PC alters the orthonormal property of the SST PCs, necessitating this pre-emptive measure.

Statistical significance of the regressions is assessed via a two-tailed Student's t-test at the 5% level using an effective sample size Ne [$=N/(1+2r_{x,1}r_{y,1}+2r_{x,2}r_{y,2}+\ldots)$, where N is time-series length; $r_{x,1}$, $r_{x,2}$...are the first, second, ...-order autocorrelations for time series x, and $r_{y,1}$, $r_{y,2}$... for time series y; Quenouille, 1952] that accounts for serial autocorrelation; stable Ne (and thus t-test) values are obtained by summing up to the fourth-order. Figure 21.3b–c show regressions where t-values (obtained with Ne) exceed the theoretical values at the 5% significance level.

21.5 Drought-period SST and precipitation reconstruction

The linear seasonal regressions of the SST principal components on contemporaneous SST and precipitation in the full record (October 1901–April 2006) constitute the building blocks in this reconstruction. Multiplication of each SST PC with its temporally fixed seasonal regression pattern, and summing the 11 contributions yields the reconstructed signal. The intra-basin PCs are temporally orthogonal (assured by the analysis method) while the inter-basin ones are nearly so (ensured by filtering of Pacific's influence from Atlantic SSTs prior to analysis); the largest inter-basin PC correlation is only 0.08, facilitating reconstruction of the SST and drought signals. A similar strategy was recently used to reconstruct the tropical cyclone counts in the Atlantic sector (Nigam and Guan, 2011).

21.5.1 SST reconstruction

The SST anomalies during drought and wet episodes are first reconstructed as a test of the reconstruction paradigm. The fidelity of the reconstruction (Fig. 21.2, right panels) attests to the efficacy of the SST analysis; although 11 basis functions are used in the reconstruction, only about half contribute significantly in any given period. The hydroclimate episodes are reconstructed next, relying on the SST–precipitation links operative in nature rather than in SST–forced dynamical models of the atmosphere.

21.5.2 Drought reconstruction

The SST-based precipitation reconstruction is remarkable, as is evident from the close correspondence of the observed and reconstructed structure at both regional and subcontinental scales in Fig. 21.4a (identical to Figure 2a in Nigam *et al.* 2011). The AMO-*Atl.* is influential over large swaths of the eastern continent, while the Pacific's influence (not shown, but approximately, middle minus bottom row) is confined to the central longitudes.

Dust Bowl

The Dust Bowl spring drought is remarkably reconstructed but the Dust Bowl summer drought proves challenging, with reconstruction over the Great Plains weaker in amplitude by as much as 50% (cf. Fig. 21.4a). The structural correspondence, including placement of focal points from the Gulf Coast to the Northern Plains, is however reasonable; the correspondence extends to precipitation surplus features.

The deficit in reconstruction of the Dust Bowl summer drought from SSTs is consistent with the potential contribution of other processes, notably, regional and upstream land-surface states and attendant interactions. It is also not inconsistent with arguments for additional inclusion of human land degradation in drought simulation (Cook *et al.*, 2009).

1950s drought

The shorter but more intense 1950s *fall* drought is apparently shaped by the Pacific's influence (~ middle minus bottom row) which accounts also for the wetness of the Pacific Northwest and Central America. The largely in-phase contribution of the Atlantic is important for drought severity over the southern Plains and the Gulf Coast, leading to nearly full accounting of the core precipitation deficit; the deficit feature over the southern tier states to the east of the Mississippi is however not fully recovered.

In contrast with the success in fall, the summer drought proves challenging – even more than the Dust Bowl summer drought (Guan, 2008). Drought reconstruction fails in the 1950s summer as this drought was generated, principally, by decadal SST variability in the Pacific and Atlantic basins, i.e. by modes having weak concurrent summer precipitation links. Canonical La Niña variability, which also contributes, has weak summer links as well (Guan, 2008). The summer precipitation deficit in the 1950s drought may thus have its origin in the unrelenting fall (and winter) precipitation deficits that were sequestered in the land surface until the following spring and summer, when they would find expression as reduced evaporation (and precipitation); a well-known moisture pathway in seasonal hydroclimate evolution (e.g., Nigam and Ruiz-Barradas, 2006).

1980s wet episode

The 1980s wet episode is quite reasonably reconstructed from the SST links, though not to the extent of the 1950s drought. The in-phase basin influences generate a realistic wet pattern, but the amplitude is recovered primarily over the Lower Mississippi.

21.5.3 Drought reconstruction: synopsis

The AMO-*Atl* contribution itself is shown in Fig. 21.4a (bottom row) and is sizeable in the spring and fall episodes.

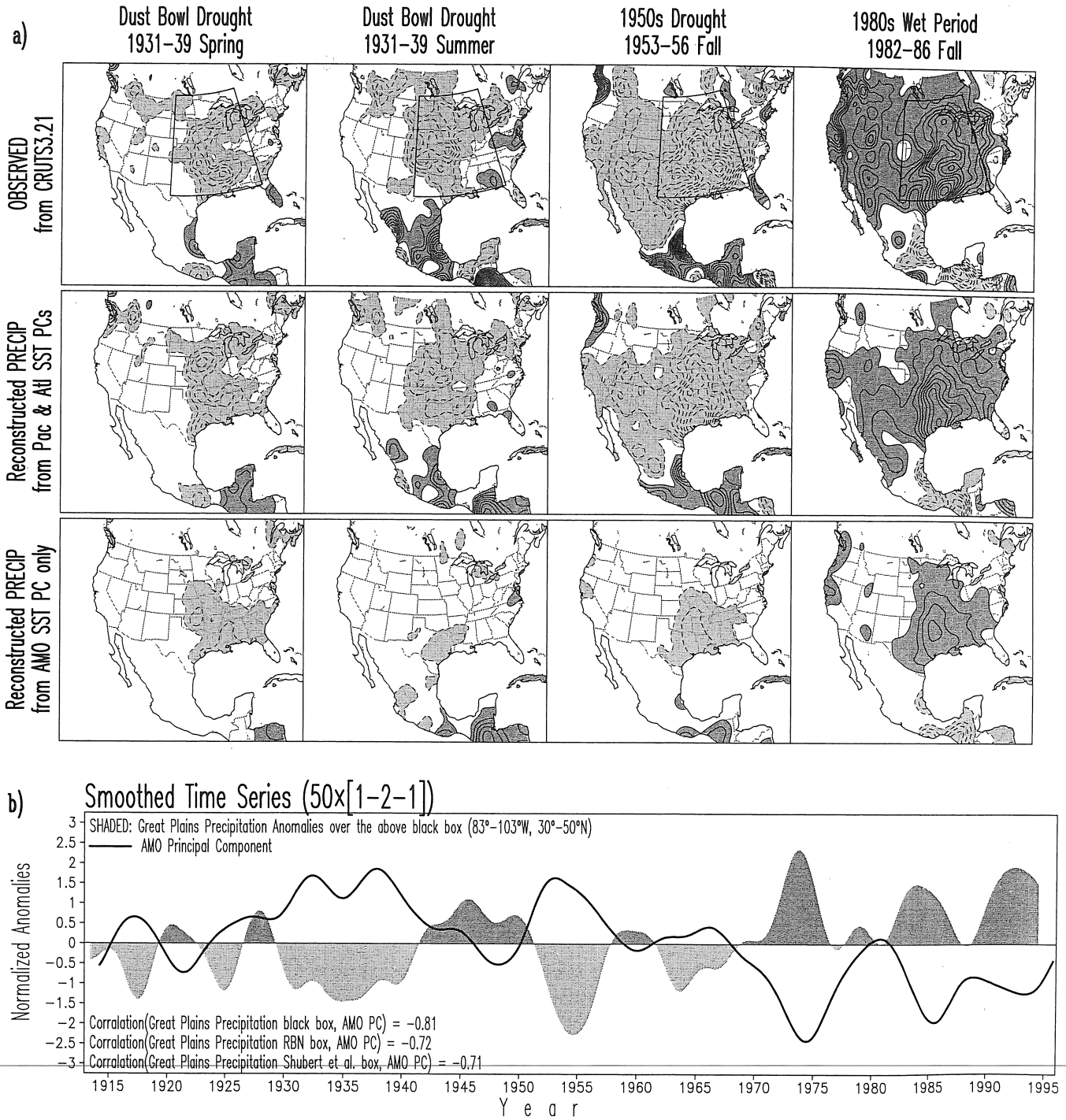

Fig. 21.4. (A) Observed (top row) and reconstructed (second row) twentieth century Great Plains droughts and wet episodes. Seasonal precipitation regressions of the seven Pacific and four Atlantic SST principal components over the October 1901–April 2006 period constitute the building blocks of the Dust Bowl (1931–39) spring and summer droughts (first and second column), 1953–56 fall drought (third column), and the 1982–86 fall wet episode (right column). The AMO-*Atl* contribution to the reconstruction is shown in the third row. Contouring, shading, and smoothing of precipitation as in Fig. 21.1e–h. The 20° wide latitude–longitude box marked in red in the top panels identifies a common impacted region; (B) Average precipitation in the marked red box is plotted along with the AMO-*Atl* SST principal component; both time series are smoothed by 50 applications of the 1-2-1 smoother on seasonal values, and normalized. The AMO-*Atl* curve is identical to that displayed in Fig. 21.3A, and is correlated with the precipitation curve at −0.78; its correlation with other precipitation averages is noted in the legend. RBN box: 100-90W, 35–45N (Ruiz-Barradas and Nigam, 2005); Schubert *et al.* box: 105–95W, 30–50N (Schubert *et al.*, 2004).

Table 21.1. *Percentage contribution of the Pacific and Atlantic SST principal components to Great Plains droughts and wet episodes; the principal components are defined and displayed in GN2008 and GN2009. The contributions are noted when the reconstructed signal is ≥10% of the observed precipitation anomaly in the 20° latitude-longitude box (103-83W, 30-50N) covering ~4 million km^2 and outlined in red in the top panels of Fig. 21.4a.*

Hydroclimate Episodes	Canonical ENSO ($ENSO^- + ENSO^+$)	ENSO Non-Canonical ($ENSO^{NC}$)	North Pacific Decadal Var. (PDV-NP)	SST Secular Trend (Nonstationary)	Atlantic Multidecadal Oscillation (AMO-*Atl*)	**Tropical Atlantic** SST Variability ($Niño^- + Niño^+$)	TOTAL (from 11 modes)
Dust Bowl Drought (***Spring*** 1931–1939) ***Deficit: 0.253 mm/day***	8			26	**55**	12ñ	92
Dust Bowl Drought (***Summer*** 1931–1939) ***Deficit: 0.291 mm/day***		9		22	12	**31**	82
1950s Drought (***Fall*** 1953–1956) ***Deficit: 0.626 mm/day***	23		**29**		24		78
1980s Wet Period (***Fall*** 1982–1986) ***Surplus: 0.687 mm/day***	14		19		**37**		75

AMO-*Atl* is dominant in Dust Bowl spring and in the 1980s wetness in the central-eastern continent (~4 million km^2 region outlined in red in the top panels of Fig. 21.4a). Interestingly, the tropical Atlantic SST modes contribute the most during Dust Bowl summer (cf. Table 21.1). The Atlantic SSTs are thus very influential in three of the four hydroclimate episodes, with the Pacific SST influence dominant only in the 1950s fall drought; a quantitative assessment of the basin contributions is given in Table 21.1 and discussed in Section 21.6.

A compelling view of AMO-*Atl*'s influence on Great Plains' hydroclimate is provided by Fig. 21.4b, which shows the normalized AMO-*Atl* SST PC (red curve) and central-eastern US precipitation in the twentieth century. Their negative correlation (−0.78) indicates an important role for the AMO in Great Plains hydroclimate variability; see also Kushnir *et al.* (2010). Together with the role of tropical Atlantic SSTs in Dust Bowl summer (noted above), this analysis suggests that, as a basin, the Atlantic is, perhaps, more influential than the Pacific for multi-year Great Plains drought and wetness.

21.6 Great Plains drought origin and predictability

A reasonable reconstruction of the major drought and wet episodes, and assessment of the Pacific and Atlantic SST contributions are prerequisite for the investigation of drought and wetness origin. In this observational analysis, the origin is investigated by resolving the basin contributions into components attributed to that basin's SST variability modes. Modal contributions are noted in Table 21.1 when they typically exceed 10% of the precipitation deficit/surplus in the red outlined box marked in Fig. 21.4a. This condition is met by canonical ENSO, non-canonical ENSO, North Pacific decadal variability, SST Secular Trend, AMO-*Atl*, and the tropical Atlantic SST modes; some of these were briefly discussed in Section 21.4, and all are fully described in GN2008 and GN2009.

21.6.1 Modal contributions

Over 90% of the Dust Bowl spring drought is reconstructed, principally, from the in-phase impact of the SST Secular Trend (~25%), AMO-*Atl* (55%), and tropical Atlantic SST modes (~10%); note, the impact of low-frequency NAO is also significant but off-setting (−15%). The Atlantic basin (tropical and extratropical) is thus quite influential for the spring drought. The drought is reconstructed to a lesser extent in summer (~80%), from non-canonical ENSO (~10%), SST Secular Trend (~20%), AMO-*Atl* (~10%), and the tropical Atlantic (30%) contributions. The Dust Bowl summer drought is thus found to be linked with tropical SST variations in the adjoining basins.

The 1950s fall drought and the 1980s fall wetness are reconstructed to an even lesser extent (~75%). The former has >20% contributions from canonical ENSO (La Niña, ~25%), PDV-NP (~30%), and AMO-*Atl* variability (warm phase, ~25%). The latter – a wet episode – is significantly influenced by canonical ENSO (El Niño, 15%), PDV-NP (~20%), and AMO-*Atl* variability (cold phase, ~35%). Both the 1950s and 1980s fall-season hydroclimate episodes, each of multi-year duration, are nominally consistent with the La Niña – US Drought paradigm, which captures the interannual influence on winter–spring precipitation. While clearly relevant, it is however not the only key SST–drought link in the fall season: Table 21.1 shows that AMO-*Atl* exerts the strongest influence in two of the four episodes (with the tropical Atlantic modes being most influential in another), indicating an important role of Atlantic SSTs in generation of multi-year drought and wet episodes over North America.

21.6.2 Drought predictability

The above reported drought reconstruction was based on contemporaneous precipitation regressions of the SST PCs, and as such, does not allow for the inference that SST variations lead to drought and wet episodes. If North American droughts were primarily linked with tropical SST variability, the SST attribution would have been more straightforward, in view of the amassed observational and modeling evidence for the regional-to-hemispherical scale influence of tropical SST anomalies; the profound impact of El Niño SSTs, for example.

The SST–drought links articulated above however involve patterns with tropical *and* extratropical SST features, necessitating further analysis of causality. That tropical features remain the real instigators of droughts, with the mid-latitude ones (shaped, to an extent, by ensuing feedbacks) exerting more modest influence, is a distinct possibility, but one that cannot be confirmed or refuted by this observational analysis or even by modeling with present-day atmospheric models, which remain challenged in simulation, let alone prediction, of regional hydroclimate variability and change.

Regardless, some insight on the role of SST is provided from reconstructing droughts with antecedent SSTs. As the hydroclimate episodes of interest have durations of 4–10 years, the reconstruction is undertaken using decadal modes of SST variability. The droughts are reconstructed in Fig. 21.5 from the SST-leading regressions on continental precipitation. The reconstruction is obtained by multiplying the decadal SST PCs with their 1–6 year lagged precipitation regressions. The coherent nascent drought signals in the SST-leading reconstructions in Fig. 21.5 (and their absence in most SST-lagged reconstructions shown in the far-right column of this figure) support the case for a causative role of SSTs in North American droughts. However, as the drought reconstruction reported in Fig. 21.5 is for periods not independent of the one used in generating the underlying building blocks (regressions), the drought/wetness reconstructed from antecedent SSTs in Fig. 21.5 cannot be considered SST-based hindcast prediction. This analysis nonetheless provides preliminary evidence for the potential predictability of droughts.

21.7 Drying of the Sahel

The declining precipitation over Sahel over a three-decade period (1950s to 1980s) remains enigmatic, as noted in the introduction. The multi-decade 'drying' is reconstructed in this section to gain insight into its causes. The drying signal is clearly manifest in the regionally averaged (20W–40E; 10N–20N) boreal summer (June–August) rainfall anomaly record (Fig. 21.6, solid black curve). The precipitous drop in precipitation from the mid 1950s to the mid 1980s (by over 1.5 mm/day) is idealized by the straight black line. The rainfall decline is very significant – leading to widespread use of the term 'drying' – as the seasonal summer rainfall over this continental strip (mostly its southern part) is 4.2 mm/day with an interannual standard deviation (SD) of 0.5 mm/day, i.e. the rainfall decline was almost 2 SD in the peak dry phase!

The Sahel rainfall record was reconstructed using Pacific and Atlantic SST PCs, just as over the Great Plains. The reconstructed rainfall (dashed black line in Fig. 21.6) tracks the observed rainfall closely (correlation 0.91), robustly capturing the drying of the Sahel and the rainfall recovery since. With the target in hand, partial rainfall reconstructions are undertaken to identify the influential modes of SST variability within the context of this analysis. Both the Atlantic and Pacific (green and blue curves respectively) are influential, albeit at different stages; Atlantic in the early and Pacific in the latter period, as indicated by the idealized green and blue straight-line drops. North Pacific decadal SST variability dominates the Pacific contribution and AMO-*Atl* the Atlantic one. Interestingly, the rainfall reconstructed from just these two modes of SST variability tracks the observed rainfall record almost as well as the full reconstruction (0.83 versus 0.91 correlation).

Statistical analysis and reconstruction often suffer from concerns related to causality and physicality in the case of analysis, and over-fitting in the case of reconstruction. The over-fitting is readily put to rest by noting that just two modes of SST variability can generate the Sahel rainfall record, including the multi-decade long drying episode and subsequent rainfall recovery. The first concern is more

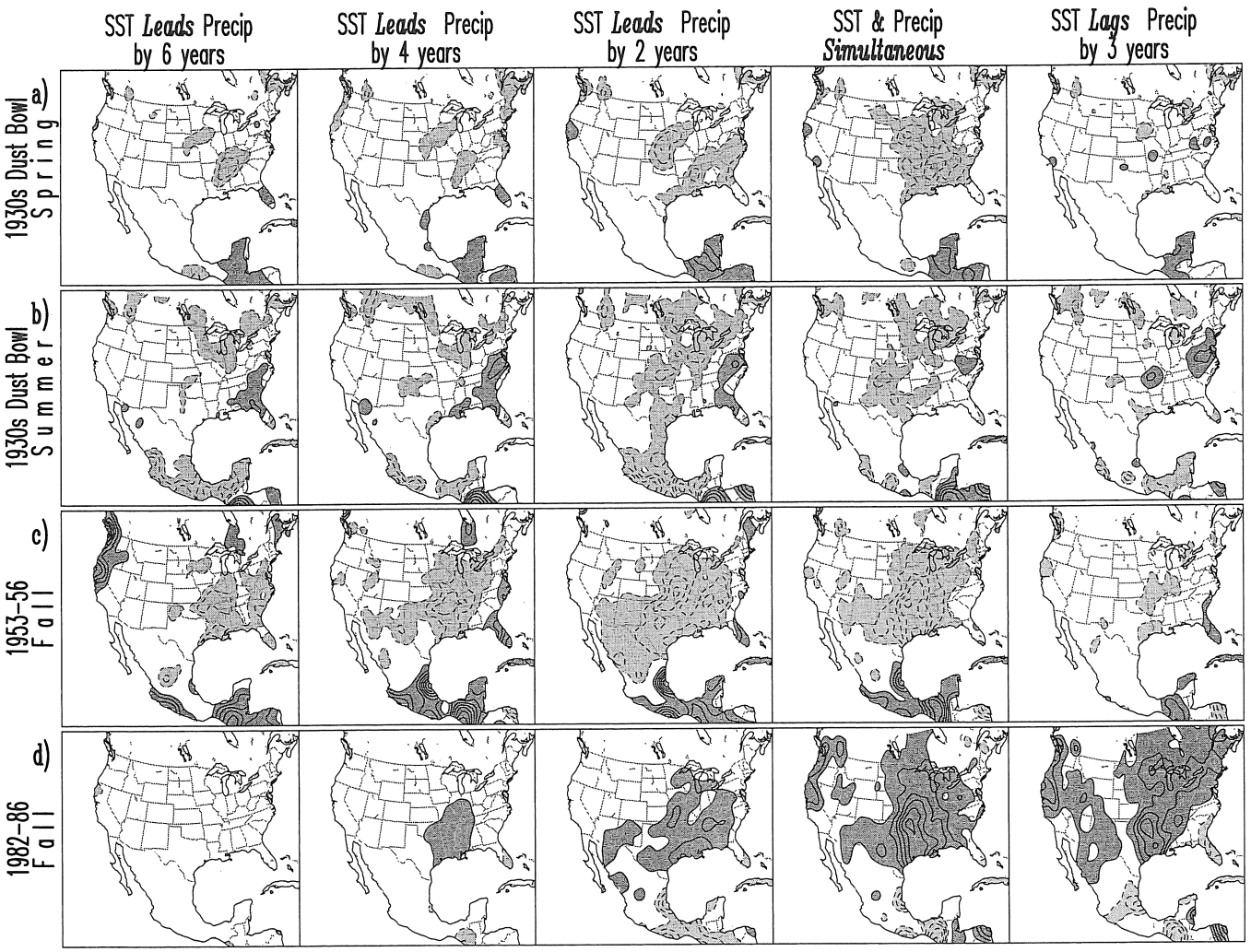

Fig. 21.5. Drought reconstruction based on SST-*leading* (and lagging) regressions of the decadal SST PCs (SST Secular Trend, PDV-North Pacific, ENSO-Non Canonical, AMO-*Atl*, and Low Frequency NAO): The SST-lead ranges from 6-to-0 years, and a 3-year SST-lag case (far right) is also shown. The drought build-up is evident with reduced SST-lead in each case. Rest as in Fig. 21.4a.

pertinent though as, unlike the Great Plains case, no follow-up analysis was presented to provide insight into the dynamical and thermodynamical processes causing the rainfall decline over the Sahel. This analysis, nonetheless, suggests that warm Atlantic SSTs (both in middle-high latitudes and the tropics-subtropics, cf. Fig. 21.3b) lead to a wetter Sahel, not a drier one; note Giannini *et al.* (2003) argue that warmer Atlantic SSTs lead to build-up of the oceanic ITCZ at the expense of the continental one, i.e. at odds with the AMO-*Atl* influence noted here.

A contemporaneous statistical link between North Pacific decadal SST variability (PDV-NP *a la* PDO) and Sahel rainfall seems more intriguing. Even if SSTs are assumed to be the cause, elaboration on the mechanism by which mid-latitude Pacific SST anomalies impact summer rainfall over northern tropical Africa would be challenging, as SST anomalies in only the Tropics are generally considered causative. Interestingly, the PDV-NP is not without tropical links, notwithstanding its name. Guan and Nigam (2008) showed PDV-NP linked with the tropical Indian and Pacific basin SSTs; see also Deser *et al.* (2004). Figure 12 of Guan and Nigam shows SST regressions and correlations of the PDV-NP SST principal component. The correlation map readily reveals the tropical links, especially in the Indian Ocean and Western Pacific, where smaller amplitudes of SST variability create a detection challenge, but not for the correlation statistic.

The Indian Ocean SST links of the PDV-NP mode both impart plausibility and indicate a potential pathway by which this mode of Indo-Pacific SST variability can influence Sahel rainfall on decadal time scales. Note, the 1960s–1980s decline in Sahel rainfall is coincident with the phase-reversal of the PDV-NP mode (from positive to negative phase; cf. Figure 2 in GN2008), i.e. coincident

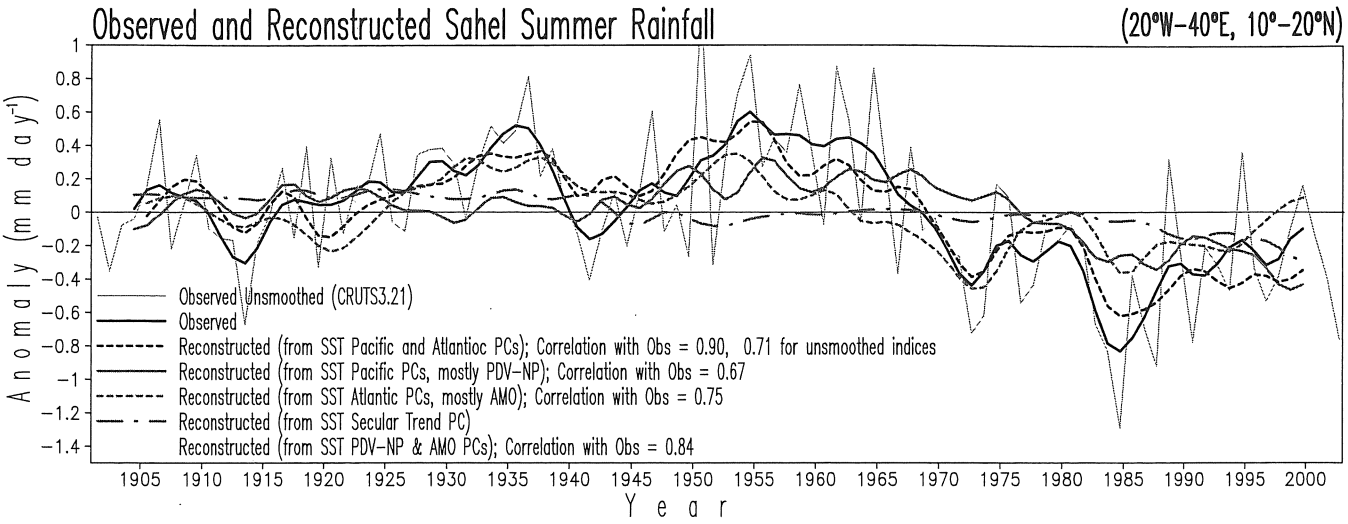

Fig. 21.6. Observed and reconstructed Sahel rainfall record. The 20W–40E and 10N–20N averaged rainfall anomaly in boreal summer (June–August) is shown during the twentieth century. Observed anomaly is depicted by the solid black line, while the Pacific and Atlantic SST based rainfall reconstruction is shown by the dashed black line (correlated at 0.91 with the observed record). The individual basin contributions to the reconstruction are in blue (Pacific) and green (Atlantic); the contribution of SST Secular Trend alone is in red. All curves have been smoothed from three applications of the 1-2-1 smoother on yearly summer data. That Sahel rainfall variations can be effectively reconstructed from just the AMO-*Atl* and PDV-NP rainfall regressions is evident from the 0.83 correlation of this reconstruction with observations, as noted in legend. Inclusion of the other nine SST principal component contributions improves the correlation only slightly, to 0.91; the correlation is 0.72 without any smoothing.

with the multidecadal warming of the tropical-subtropical Indian Ocean basin. The competition between continental (African and Indian) and oceanic (Indian basin) convection could be a mechanism underlying the statistical link between Sahel rainfall and North Pacific (and Indian Ocean) decadal SST variability.

21.8 Concluding remarks

Droughts (and wet episodes) over the Great Plains have been linked to SST variability in the Pacific and Atlantic basins. The basin influences have however yet to be fully evaluated, in part, because the SST-forced dynamical models of the atmosphere – a common investigative tool – remain challenged in simulation of regional hydroclimate variability; the specification of SST anomalies in the models' extratropics may be problematic as well (Kushnir *et al.*, 2002).

Here we adopt a statistical approach rooted in spatio-temporal (extended-EOF) analysis of twentieth century SST variations (GN2008, GN2009) and related drought links (Guan, 2008), which leads to impressive reconstruction of several (but not all) major droughts and wet episodes; attesting to the extent of the SST influence on Great Plains hydroclimate in nature. We find Atlantic SSTs, tropical, and extratropical, to be particularly influential; often, more than the Pacific ones, and more than indicated in previous analyses (especially those based on SST-forced atmospheric models): AMO is the dominant contributor in the Dust Bowl spring drought and in the 1980s fall wetness (i.e. in two of the four episodes), while tropical Atlantic SST variability is in another (Dust Bowl summer). As a basin, the Atlantic is more influential than the Pacific in three of the four reconstructed episodes (cf. Table 21.1).

The AMO's influence on continental hydroclimate is provided circulation context from analysis of low-level flow and column stationary moisture flux, both obtained from NOAA's Twentieth Century Reanalysis. The modulation of moisture transport is important, especially in fall when AMO's impact on Great Plains precipitation is strongest. A hypothesis for how the AMO atmospheric circulation anomalies are generated from AMO SSTs was proposed by Nigam *et al.* (2011) to advance discussion of the influence pathways of the mid-to-high latitude SST anomalies.

The Atlantic SSTs evidently exert a profound influence on Great Plains hydroclimate on decadal time scales, especially in the transition seasons; an influence not represented in the SST-forced dynamical models of the atmosphere. For instance, Schubert *et al.* (2009) find a cold Pacific and neutral Atlantic to be significantly more influential for US droughts than a neutral Pacific and warm Atlantic

(PcAn>>PnAw in their drought modeling experiment nomenclature).

Our analysis suggests that the La Niña – US drought paradigm – operative on interannual time scales in nature – has been conferred excessive relevance on decadal time scales in the recent literature, in part, because dynamical models of the atmosphere are unable to represent the influence of Atlantic SSTs on Great Plains hydroclimate.

With respect to multidecadal rainfall variations over Sahel, including the drying of Sahel in the 1950s to 1980s, our statistical analysis indicates an important role for both AMO-*Atl* and Indo-Pacific decadal SST variability (PDV-NP). The dynamical and thermodynamical mechanisms underlying these links need elaboration, but a potential influence pathway is briefly discussed.

Regardless, the present analysis is encouraging for the investigation of the SST-based experimental statistical decadal prediction of North American and African droughts, complementing related dynamical predictions.

21.9 Acknowledgments

The reported analysis draws heavily – text and figures – on the authors' prior publication: Nigam, S., B. Guan, and A. Ruiz-Barradas (2011): Key role of the Atlantic Multidecadal Oscillation in 20th century drought and wet periods over the Great Plains. *Geophys. Res. Lett.*, **38**, L16713, doi:10.1029/2011GL048650.

A.B. contributed to data set development and the preliminary analysis of Pacific SST variability. Bin Guan refined and extended the Pacific analysis, performed the Atlantic SST analysis, and extracted the SST-drought links, all as part of his doctoral dissertation to the University of Maryland (defended October 2008). S.N. formulated the research design, refined the analysis strategy, conducted the column moisture-flux analysis, and developed the manuscript.

References

Barlow, M., S. Nigam, and E. Berbery (2001). ENSO, Pacific decadal variability, and US summertime precipitation, drought, and stream flow. *Journal of Climate* **14**(9), 2105–2128.

Biasutti, M., *et al.* (2008). SST forcings and Sahel rainfall variability in simulations of the twentieth and twenty-first centuries. *Journal of Climate* **21**(14), 3471–3486.

Charney, J. (1976). Dynamics of deserts and drought in Sahel-Reply. *Quarterly Journal of the Royal Meteorological Society* **102**(432) 468–468.

Charney, J. and P. Stone (1976). Drought in Sahara – Insufficient biogeophysical feedback. *Science* **191**(4222), 100–102.

Compo, G., *et al.* (2011). The twentieth century reanalysis project. *Quarterly Journal of the Royal Meteorological Society* **137**(654), 1–28.

Cook, B., R. Miller, and R. Seager (2009). Amplification of the North American "Dust Bowl" drought through human-induced land degradation. *Proceedings of the National Academy of Sciences of the United States of America* **106**(13), 4997–5001.

Dai, A., K. Trenberth, and T. Qian (2004). A global dataset of Palmer Drought Severity Index for 1870–2002: Relationship with soil moisture and effects of surface warming. *Journal of Hydrometeorology* **5**(6), 1117–1130.

Deser, C., A. Phillips, and J. Hurrell (2004). Pacific interdecadal climate variability: Linkages between the tropics and the North Pacific during boreal winter since 1900. *Journal of Climate* **17**(16), 3109–3124.

Enfield, D. and L. Cid-Serrano (2010). Secular and multidecadal warmings in the North Atlantic and their relationships with major hurricane activity. *International Journal of Climatology* **30**(2), 174–184.

Enfield, D., A. Mestas-Nunez, and P. Trimble (2001). The Atlantic multidecadal oscillation and its relation to rainfall and river flows in the continental US. *Geophysical Research Letters* **28**(10), 2077–2080.

Folland, C., T. Palmer, and D. Parker (1986). Sahel rainfall and worldwide sea surface temperatures, 1901–85. *Nature* **320** (6063) 602–607.

Giannini, A., R. Saravanan, and P. Chang (2003). Oceanic forcing of Sahel rainfall on interannual to interdecadal time scales. *Science* **302**(5647) 1027–1030.

Guan, B. (2008). Pacific sea surface temperatures in the twentieth century: Variability, trend, and connections to long-term hydroclimate variations over the Great Plains, *Ph.D. thesis*, 116 pp., Univ. of Maryland, College Park.

Guan, B. and S. Nigam (2008). Pacific sea surface temperatures in the twentieth century: An evolution-centric analysis of variability and trend. *Journal of Climate* **21**(12), 2790–2809.

Guan, B. and S. Nigam (2009). Analysis of Atlantic SST variability factoring interbasin links and the secular trend: Clarified structure of the Atlantic Multidecadal Oscillation. *Journal of Climate* **22**(15), 4228–4240.

Hare, S. and N. Mantua (2000). Empirical evidence for North Pacific regime shifts in 1977 and 1989. *Progress in Oceanography* **47**(2-4), 103–145.

Held, I., *et al.* (2005). Simulation of Sahel drought in the 20th and 21st centuries. *Proceedings of the National Academy of Sciences of the United States of America* **102**(50), 17891–17896.

Huang, J., H. vandenDool, and K. Georgakakos (1996). Analysis of model-calculated soil moisture over the United States (1931–1993) and applications to long-range temperature forecasts. *Journal of Climate* **9**(6), 1350–1362.

Hulme, M. (1992). Rainfall changes in Africa – 1931–1960 to 1961–1990. *International Journal of Climatology* **12**(7) 685–699.

Joseph, R. and S. Nigam (2006). ENSO evolution and teleconnections in IPCC's twentieth-century climate simulations:

Realistic representation? *Journal of Climate* **19**(17) 4360–4377.

Kalnay, E., *et al.* (1996). The NCEP/NCAR 40-year reanalysis project. *Bulletin of the American Meteorological Society* **77**(3), 437–471.

Kushnir, Y., *et al.* (2002). Atmospheric GCM response to extratropical SST anomalies: Synthesis and evaluation. *Journal of Climate* **15**(16), 2233–2256.

Kushnir, Y., *et al.* (2010). Mechanisms of tropical Atlantic SST influence on North American precipitation variability. *Journal of Climate* **23**(21), 5610–5628.

McCabe, G., *et al.* (2008). Associations of multi-decadal sea-surface temperature variability with US drought. *Quaternary International* **188** 31–40.

McCabe, G., M. Palecki, and J. Betancourt (2004). Pacific and Atlantic Ocean influences on multidecadal drought frequency in the United States. *Proceedings of the National Academy of Sciences of the United States of America* **101**(12), 4136–4141.

Mitchell, T. and P. Jones (2005). An improved method of constructing a database of monthly climate observations and associated high-resolution grids. *International Journal of Climatology* **25**(6), 693–712.

Mo, K., J. Schemm, and S. Yoo (2009). Influence of ENSO and the Atlantic Multidecadal Oscillation on Drought over the United States. *Journal of Climate* **22**(22) 5962–5982.

Namias, J. (1966). Nature and possible causes of northeastern United States drought during 1962–65. *Monthly Weather Review* **94**(9), 543–554.

Nigam, S. and B. Guan (2011). Atlantic tropical cyclones in the twentieth century: natural variability and secular change in cyclone count. *Climate Dynamics* **36**(11–12), 2279–2293.

Nigam, S., B. Guan, and A. Ruiz-Barradas (2011). Key role of the Atlantic Multidecadal Oscillation in 20th century drought and wet periods over the Great Plains. *Geophysical Research Letters* **38**.

Nigam, S. and A. Ruiz-Barradas (2006). Seasonal hydroclimate variability over north America in global and regional reanalyses and AMIP simulations: Varied representation. *Journal of Climate* **19**(5), 815–837.

Nigam, S., M. Barlow, and E. H. Berbery (1999). Analysis links Pacific decadal variability to drought and streamflow in United States, *Eos Trans. AGU*, **80**, 621–625, doi:10.1029/99EO00412.

Quenouille, M. H. (1952). *Associated Measurements*, Academic, New York.

Palmer, W. C. (1966). Meteorological drought. *U.S. Weather Bureau Tech. Paper 45*, 58 pp. Available from NOAA/National Weather Service, 1325 East-West Highway, Silver Spring, MD 20910.

Rasmusson, E. and T. Carpenter (1983). The relationship between eastern equatorial Pacific sea-surface temperatures and rainfall over India and Sri-Lanka. *Monthly Weather Review* **111**(3) 517–528.

Rayner, N., *et al.* (2003). Global analyses of sea surface temperature, sea ice, and night marine air temperature since the late nineteenth century. *Journal of Geophysical Research-Atmospheres* **108**(D14).

Ropelewski, C. and M. Halpert (1987). Global and regional scale precipitation patterns associated with the El Niño Southern Oscillation. *Monthly Weather Review* **115**(8) 1606–1626.

Ruiz-Barradas, A. and S. Nigam (2005). Warm season rainfall variability over the US great plains in observations, NCEP and ERA-40 reanalyses, and NCAR and NASA atmospheric model simulations. *Journal of Climate* **18**(11) 1808–1830.

Ruiz-Barradas, A. and S. Nigam (2010a). Great Plains precipitation and its SST links in twentieth-century climate simulations, and twenty-first- and twenty-second-century climate projections. *Journal of Climate* **23**(23), 6409–6429.

Ruiz-Barradas, A. and S. Nigam (2010b). SST-North American Hydroclimate Links in AMIP Simulations of the Drought Working Group Models: A Proxy for the Idealized Drought Modeling Experiments. *Journal of Climate* **23**(10), 2585–2598.

Ruiz-Barradas, A. and S. Nigam (2013). Atmosphere-land surface interactions over the Southern Great Plains: Characterization from pentad analysis of DOE ARM field observations and NARR. *Journal of Climate* **26**(3), 875–886.

Schubert, S., *et al.* (2009). A US CLIVAR project to assess and compare the responses of global climate models to drought-related SST forcing patterns: Overview and results. *Journal of Climate* **22**(19) 5251–5272.

Schubert, S., *et al.* (2004). Causes of long-term drought in the US Great Plains. *Journal of Climate* **17**(3) 485–503.

Seager, R., *et al.* (2005). Modeling of tropical forcing of persistent droughts and pluvials over western North America: 1856–2000. *Journal of Climate* **18**(19) 4065–4088.

Slonosky, V., L. Mysak, and J. Derome (1997). Linking Arctic sea-ice and atmospheric circulation anomalies on interannual and decadal timescales. *Atmosphere-Ocean* **35**(3), 333–366.

Sutton, R. and D. Hodson (2005). Atlantic Ocean forcing of North American and European summer climate. *Science* **309**(5731), 115–118.

Ting, M., *et al.* (2009). Forced and internal twentieth-century SST trends in the North Atlantic. *Journal of Climate* **22**(6), 1469–1481.

Ting, M. and H. Wang (1997). Summertime US precipitation variability and its relation to Pacific sea surface temperature. *Journal of Climate* **10**(8), 1853–1873.

van den Dool, H., J. Huang, and Y. Fan (2003). Performance and analysis of the constructed analogue method applied to US soil moisture over 1981–2001. *Journal of Geophysical Research-Atmospheres* **108**(D16).

von Storch H. and F. W. Zwiers (1999). *Statistical Analysis in Climate Research*. Cambridge University Press, 494 pp.

Wang, C., *et al.* (2006). Influences of the Atlantic warm pool on western hemisphere summer rainfall and Atlantic hurricanes. *Journal of Climate* **19**(12), 3011–3028.

Weare, B. and J. Nasstrom (1982). Examples of extended empirical orthogonal function analyses. *Monthly Weather Review* **110**(6), 481–485.

Weaver, S. and S. Nigam (2008). Variability of the great plains low-level jet: Large-scale circulation context and hydroclimate impacts. *Journal of Climate* **21**(7), 1532–1551.

White, W. B., A. Gershunov, and J. Annis (2008). Climatic influences on Midwest drought during the twentieth century, *Journal of Climate* **21**, 517–553.

Zhang, R. and T. Delworth (2006). Impact of Atlantic multidecadal oscillations on India/Sahel rainfall and Atlantic hurricanes. *Geophysical Research Letters* **33**(17).